Si nanowire metal–insulator–semiconductor photodetectors as efficient light harvesters

2010 Nanotechnology 21 095502

(http://iopscience.iop.org/0957-4484/21/9/095502)

Nanotechnology **21** (2010) 095502 (5pp) doi:10.1088/0957-4484/21/9/095502

Si nanowire metal–insulator–semiconductor photodetectors as efficient light harvesters

Joonho Bae[1,6], Hyunjin Kim[2,6], Xiao-Mei Zhang[1,3], Cuong H Dang[2], Yue Zhang[3], Young Jin Choi[4,5], Arto Nurmikko[2] and Zhong Lin Wang[1]

[1] School of Materials Science and Engineering, Georgia Institute of Technology, Atlanta, GA 30332, USA
[2] Division of Engineering and Department of Physics, Brown University, Providence, RI 02912, USA
[3] Department of Materials Physics and Chemistry, University of Science and Technology Beijing, Beijing 100083, People's Republic of China
[4] Department of Physics, MyongJi University, Yongin 449-728, Korea
[5] Department of Nano Science and Engineering, MyongJi University, Yongin 449-728, Korea

E-mail: Arto_Nurmikko@brown.edu and zlwang@gatech.edu

Received 9 October 2009, in final form 11 January 2010
Published 4 February 2010
Online at stacks.iop.org/Nano/21/095502

Abstract
Novel ITO-Si nanowire (NW) metal–insulator–semiconductor (MIS) photodetectors were fabricated by using n-type Si NWs as detection units and ITO films as top gate electrodes. Measurements on the Si NW based device reveal a significant photoresponse, including photocurrent generation with an external quantum efficiency (EQE) of ∼35% at a peak wavelength of 600 nm at zero external bias, and with an EQE of 70% at a peak wavelength of 800 nm at −0.5 V bias. The NW device shows a flat and low reflectance and almost constant EQE up to a 60° incident angle of illumination, demonstrating efficient visible-light harvesting by the Si NW antenna.

(Some figures in this article are in colour only in the electronic version)

1. Introduction

In recent years, semiconductor nanowires (NWs) have attracted much attention due to their interesting physical properties for possible applications in electronics and photonics [1–8]. In photonics applications, silicon plays a major role in photodetection and photovoltaics. Therefore, the inclusion of Si NWs in Si-based photodetectors or solar cells is of interest due to enhanced light–matter interaction and modulated interface geometry such as those offered by a core–shell junction or an enlarged junction area [9–18].

When compared with thin film Si, amorphous Si NWs and Si nanocones have been reported to exhibit effective 'antireflection' over a wide range of wavelengths and angles of incidence (AOI) [19]. This property arises from the interactions of photons in the densely packed NW environment where light scattering on a subwavelength scale can efficiently trap photons. The consequent enhancement of absorption by Si NWs could allow for low cost production of photonic devices, where these types of light-capturing coatings are part of a monolithic Si photodetector. So far, challenges in the fabrication of nano-materials and a lack of understanding of their surface electronic properties may have hindered taking full advantage of their enhanced optical properties.

In this paper we report how Si NW arrays can be monolithically incorporated into novel metal–insulator–semiconductor (MIS) photodetectors, in which ITO is used as the top transparent electrode contact to oxidized NWs. We quantify the enhancement in optical absorption of Si NWs by direct experimental comparison of them with the same type of planar Si MIS and commercial p–i–n photodetectors.

[6] These two authors contributed equally to this work.

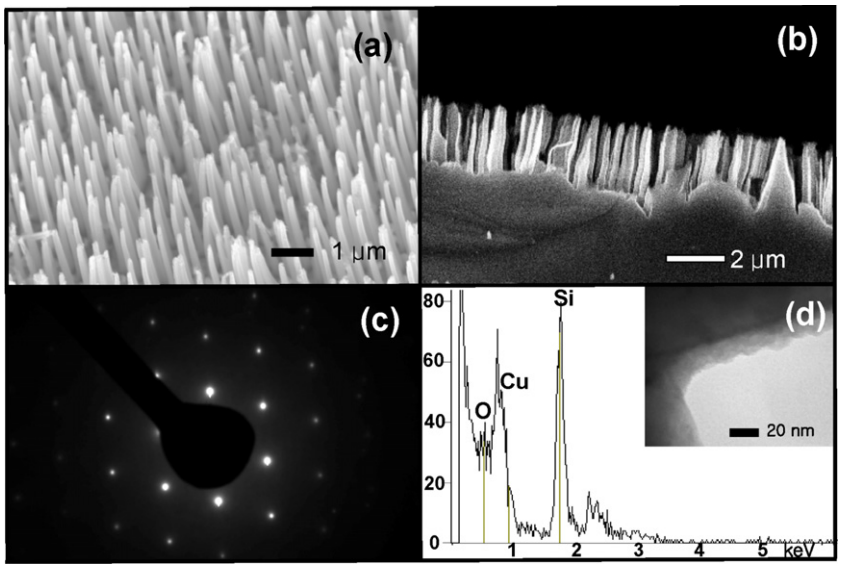

Figure 1. (a) SEM image of as-grown Si NW arrays. (b) Cross-sectional SEM image of as-grown Si NW arrays. (c) Electron diffraction pattern of a single Si NW. (d) EDS spectrum of Si oxide. Inset: low resolution TEM image of a sidewall of the Si NW.

As shown below, in addition to their robust photoresponse, our Si NW photodetectors maintained high external quantum efficiencies (EQEs) up to large AOI, suggesting that NWs might find unique applications for efficient and stable light harvesting.

2. Experimental details

In order to fabricate the NW MIS photodetectors, Si NW arrays were fabricated using template-assisted chemical etching [20] of a n-type Si(100) wafer with a resistivity of 5–30 Ω cm. The substrates were cut into 1 cm × 1 cm pieces, cleaned with acetone and deionized water and then heated in RCA solution ($NH_3/H_2O_2/H_2O$ 1:1:5 (v/v/v)) at 90 °C for 30 min to ensure a hydrophilic surface. A solution of polystyrene (PS) spheres with nominal diameters of 500 nm (Duke Scientific, Inc.) was diluted with ethanol with a volume ratio of 1:2, and the diluted PS/ethanol solution was placed on the substrates to obtain a large-area, close-packed monolayer of PS spheres as an etch mask, with evaporation of the solvent.

To control the diameters of the NWs, the substrate areas with coverage of close-packed PS spheres were first treated with oxygen plasma. The total pressure of the plasma chamber was ∼200 mTorr after flowing oxygen gas, and the applied RF power was 50 W. For the duration of the O_2 etching process (∼20 min), the final diameters of PS spheres were ∼200 nm. Next, a thin catalyst film of Ag (40 nm thick) was deposited on the substrate using magnetron sputtering. Then, the samples were immersed in an etching mixture of HF and H_2O_2 for 45 min at room temperature to form the NW arrays. After the etching process, the samples were immersed in toluene for 10 min to remove the remaining PS bead materials, followed by treatment in boiling aqua regia (HCl/HNO_3 3:1 v/v) to remove residual Ag film. Scanning electron microscopy (SEM) and transmission electron microscopy (TEM) were used to characterize the as-grown Si NW samples.

3. Results and discussion

Figure 1 shows electron microscope images of dense arrays of Si NWs used as a base structure for the NW photodetectors. As can be seen in figures 1(a) and (b), the NWs are highly ordered in dense arrays; each NW is ∼200 nm thick and ∼1–2 μm long. The diameter of the NWs (200 nm) is controlled by reducing the size of PS spheres in the oxygen plasma and the center-to-center distance between the NWs is determined by the diameter of the PS spheres, which is 500 nm [20]. High resolution TEM from a single NW reveals its single crystal structure with a [100] direction (figure 1(c)). Energy dispersive spectroscopy (EDS) and TEM on the single NW show a 'native' Si oxide layer (<20 nm thick) at the surface (figure 1(d) and its inset). The relatively large thickness of the oxide layer can be attributed to the chemistry of oxidization associated with the RCA cleaning process (treatment in a solution of $NH_3/H_2O_2/H_2O$) of the Si substrates before the formation of NWs.

To fabricate ITO-Si NW photodetectors, the as-grown Si NWs were next coated with ITO films with a magnetron sputter system. The thickness of the ITO film was 170 nm and the device was annealed at 350 °C to enhance the transparency of the ITO film. Ga/In alloy was attached on the rear side of the device to serve as an ohmic contact. On the top of the device (ITO side), silver paste (Ted Pella, Inc.) was used to make an ohmic contact with an Au wire. The anticipated mechanism of photocurrent generation at the planar ITO/SiO_2/Si MIS interfaces is presumed to rely on tunneling of the photo-generated holes through the thin native oxide layer to reach the metal gate, while the electrons move to the back contact by a drift and diffusion process [21]. In the case of nanoscale structures such a model may be subject to further study.

The device schematic and SEM images of our ITO-Si NW photodetector are shown in figure 2. An optical photograph of a silicon wafer and an as-grown NW substrate is added as

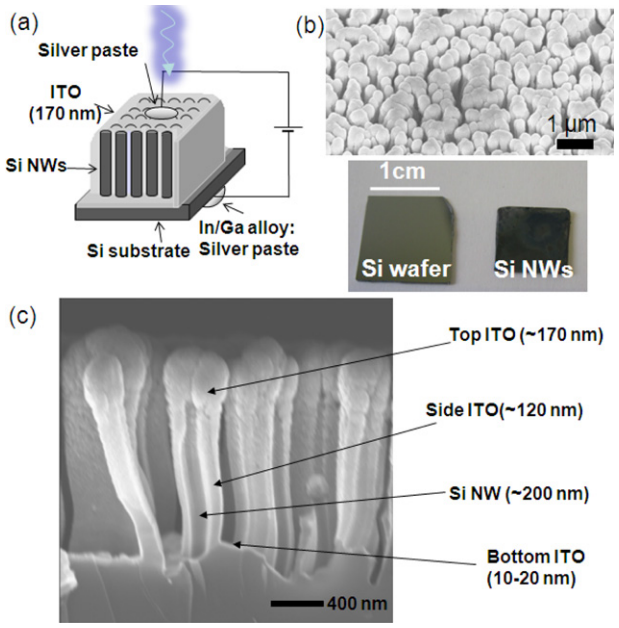

Figure 2. (a) Structural schematic of ITO/n-Si NW photodetector, and (b) planar SEM image of ITO/n-Si NWs. The inset: a photographic image of Si wafer and Si NWs. (c) Cross-sectional SEM view of ITO/n-Si NWs.

an inset to figure 2(b). The transparent ITO top contact film (thickness ∼170 nm) was deposited by vacuum sputtering to provide the electrical connection between Si NWs and ready access to top illumination. The top view SEM image in figure 2(b) suggests that the ITO film provided a reasonable coverage of the active device area where Si NWs were formed on the substrate. However, this SEM image does not show in detail what the actual contact (interface) area is for the ITO with respect to the NW arrays, i.e. to what depth the ITO reaches. As part of our ongoing investigations of the nanoscale details of the ITO contact, figure 2(c) shows a cross sectional view which suggests that, while the top regions of the SiO_2 are well covered by ITO, a thin layer of ITO reaches into the 'valleys' of the nanostructure as well.

In order to understand the lateral electrical connection of the device, we performed lateral transport measurements on the top gate ITO electrode using a four-point probe. The I–V characteristics of lateral probing exhibited ohmic behavior, indicating that lateral electrical connection of ITO was fully accomplished by conformal deposition of ITO. The sheet resistance of the ITO layer is 270 Ω/sq, exhibiting higher resistance than that of a planar ITO layer (10 Ω/sq). The relatively large lateral sheet resistance of ITO on NWs can be attributed to the relatively thinner ITO deposition on the bottom side of NWs, and perhaps the lack of a truly continuous lateral electrical pathway across the macro-scale ITO film—the details remain unclear from the purely structural image of figure 2(c). This suggests that further control of the ITO deposition is required for understanding the relative roles of the Si NWs and the Si substrate in terms of the optical and optoelectronic functions, respectively, as well as enhancement of the device performance.

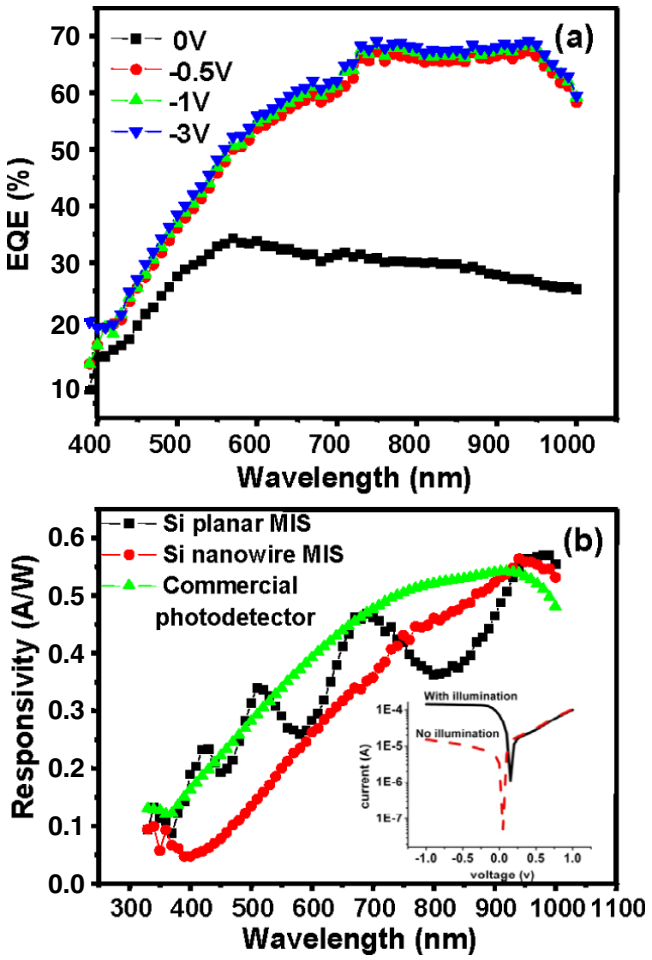

Figure 3. Characterization of the ITO/n-Si NW photodetector. (a) Spectral response from $V = 0$ to -3 V bias. (b) Comparison of the NW detector with a corresponding planar device, and a commercial Si p–i–n photodiode with comparable active areas. The inset shows the IV characteristics of NW devices in the dark and with illumination.

The ITO-Si NW devices were characterized by measuring their photocurrent spectrum (taken with a 150 W halogen lamp illuminated on the ITO side of the device with the wavelength being swept through a monochromator while recording the photocurrent). The intensity of the halogen lamp was calibrated by using a large-area commercial Si photodiode (Newport, Si-818UV, EQE of about 80% at 600 nm) for the extrapolation of the EQE and sensitivity of MIS NW devices. Figure 3(a) shows the photocurrent response of a Si NW device at four different bias voltages. The data were acquired at slow speeds, with the incident illumination amplitude modulated at 100 Hz. Note that even for zero external bias ('photovoltaic mode'), a significant photocurrent is generated with an estimated EQE of 35% at the peak response wavelength (600 nm), which indicates that the separation of photo-generated electron–hole pairs takes place in the depletion region by a built-in field. In contrast to a standard Si photodiode, we found that the present ITO-Si NW device showed an optimum response at a reverse bias of -0.5 V (with an EQE of 70% at 800 nm), beyond

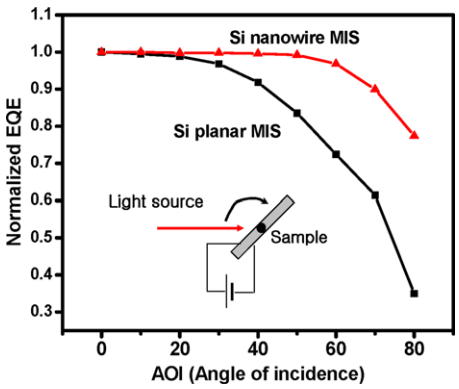

Figure 4. Plot of normalized EQE as a function of the AOI.

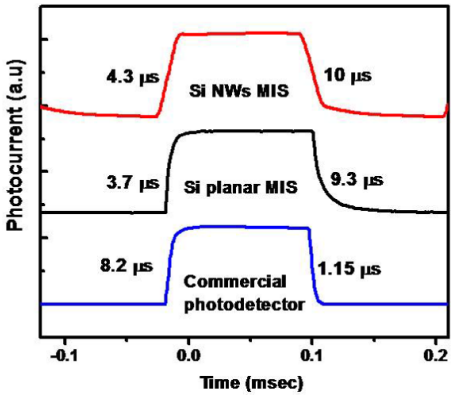

Figure 5. Response time of the Si NW photodetector, Si planar MIS photodetector, and a commercial photodetector measured by laser with 0 V reverse bias.

which the photocurrent was maintained at approximately the same level with further bias increase. In addition to using a commercial p–i–n photodetector as a direct comparison, we also fabricated a 'control device' by using a n-Si planar wafer instead of Si NWs as an active medium. Except for the difference in detection units (NWs versus planar wafer), the two devices were fabricated using the same process flow and device parameters, such as the ITO thickness, sample preparation process and the same front/back metal contact. The spectral responsivities (in units of A W^{-1}) of the ITO-Si NW device, its planar version, and the planar commercial photodetector, respectively, are summarized in figure 3(b) (note the optical interference fringes in the planar ITO-Si device). A comparable amount of photocurrent was extracted from the Si NW MIS structure when compared with both the planar MIS and p–n structures. The seemingly efficient photoresponse from these initial NW MIS devices suggests that the Si NWs appear to act as an effective light harvesting system and that the top electrical contact to the NWs by the ITO layer is reasonably conformal and laterally continuous (figure 2(b)), offering a reasonable electronic interface and path for charge extraction to an external circuit. The responsivity of the Si NW photodetector is slightly lower than that of the commercial MIS photodetector, suggesting the need for further device optimization of the NW device. The inset in figure 3(b) shows the IV characteristics of NW devices in the dark and with illumination, exhibiting a rectification ratio of 10 at ± 1 V.

For measuring the photocurrent response to varying incident AOI, the Si NW device and planar Si device were mounted on a rotatable sample holder. A continuous laser with a wavelength of 688 nm illuminated the front side of the device under identical intensities. A comparison of angular dependence of the EQEs of a NW MIS device and a planar MIS device is shown in figure 4. Note the contrast in the behavior of normalized EQEs when the angle of incident light was changed from 0° to 80°. The NW device shows a flat EQE response as the AOI is increased, remaining nearly constant up to an AOI of 60°, whereas that of the EQE of planar Si device decreased 'normally', exhibiting a 30% decrease at a 60° AOI. The improved angular response could enable the NW photodetectors to achieve more efficient harvesting of photons covering large solid AOI.

The dynamical response of the NW device was investigated by recording the photocurrent signals directly on an oscilloscope while illuminating the device by pulsed laser light (emission at 405 nm, pulsed current source ILX lightwave LDP-3811). Comparison of the response time between the NW device, Si planar MIS photodetector and a commercial Si p–i–n photodetector of comparable lateral area is shown in figure 5. The NW device shows a reasonably fast response time (approximately 4.3 μs rise time and 10 μs decay time), compared with that of the commercial device (8.2 μs rise time and 1.15 μs decay time) and Si planar MIS photodetector (3.7 μs rise time and 9.3 μs decay time), all measured under identical illumination conditions. The reasonably fast response time of the NW photodetector indicates that the enhanced surface area of the NW device is not significantly inhibiting the operation speed of the device (e.g. due to additional capacitances by the complex nanoscale contours).

In order to identify the purely optical component of the overall mechanism for the performance of the NW device, we performed measurements on the as-grown Si NWs in comparison with planar Si wafers. The hemispherical reflectance (diffuse + specular reflectance) of Si NWs and companion polished Si wafers was measured using an integrating sphere (IS) over a broad range of wavelengths (400–1000 nm) at 8° AOI. The result, as illustrated in figure 6(a), shows that the Si NWs exhibit a ~6% reflectance over a broad range of wavelengths, significantly smaller than that of the planar Si wafer (~33%). The low reflectance of silicon NWs is probably the result of two factors. Firstly, it is due to the low effective refractive index of the NW 'layer', which can be calculated from the ratio of the volume of Si NWs to that of air in the NW region (as inset in figure 6(b)) [22, 23]. The effective refractive index of the Si NW layer is estimated to be $n \sim 1.8$, which is significantly lower than that of bulk Si (3.8). Secondly, the scattering within the subwavelength size NW active 'photonic antenna' layer is expected to increase the optical reabsorption within Si NWs from an altered photon mean free path. Figure 6(b) shows the *specular* reflectance of planar and NW silicon wafers at an AOI of 7°. The specular reflectance of the Si NW is less than 0.007% in the visible region (400–800 nm) and less than 0.05% in the IR region

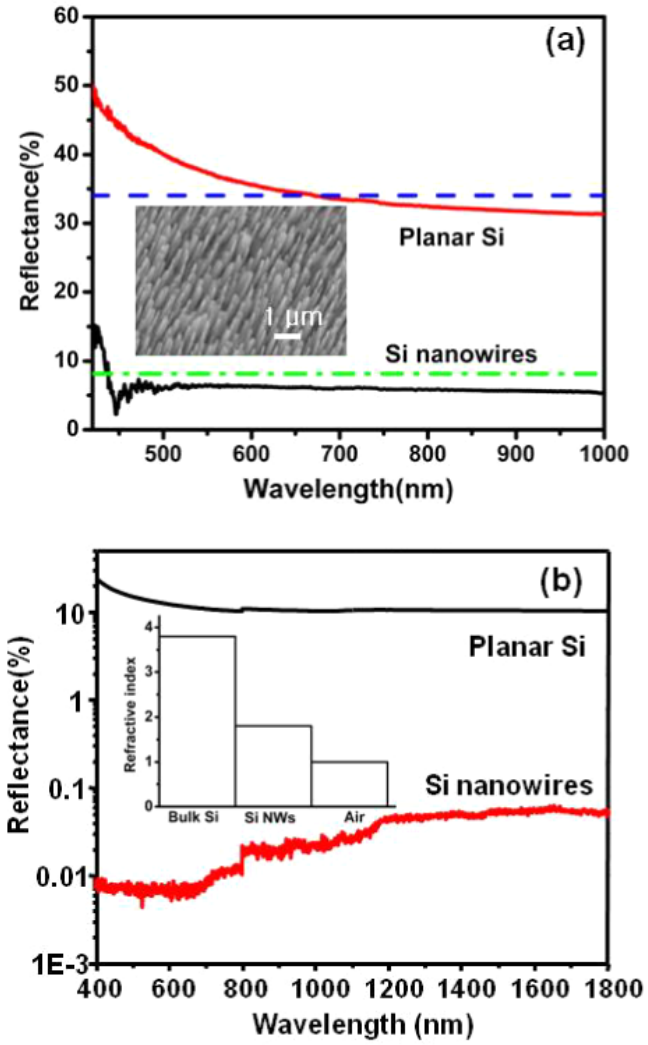

Figure 6. Comparison of the optical properties of Si NWs and planar n-Si wafers. (a) The hemispherical reflectance (diffuse + specular reflectance) of Si NWs and Si wafers. The blue dotted line and green dotted line correspond to calculated reflectances of planar Si and Si NWs using their refractive index (planar Si, 3.8; Si NWs, 1.8). (b) The specular reflectance of planar and NW silicon wafers at an AOI of 7°. (c) The inset is the effective refractive index of the NW region.

(800–1800 nm), which is two orders of magnitude smaller than the angularly integrated hemispherical reflectance.

4. Conclusions

In summary, novel ITO-Si NW MIS photodetectors were fabricated using n-Si NWs as substrates and ITO films as gate electrodes. The devices show a very reasonable photoresponse; for example, a significant photocurrent is generated with an EQE of 35% at a peak wavelength of 600 nm without bias. The NW devices show a rather flat EQE response as a function of the incident angle of illumination when compared with planar Si p–i–n photodetectors. Basic optical measurements show how the NW arrays act as an effective means to couple more illumination to the structures. However, at this point in our work it remains unclear what fraction of the overall photodetector efficiency is actually contributed directly by the photoelectronic conversion pathway in the NWs themselves, as opposed to the role of the Si substrate in the process. In principle, providing a continuous photoelectronic landscape across the entire NW array surface should offer significant further improvement of these types of 'hybrid' subwavelength optical and nanoelectronic devices.

Acknowledgments

Research was supported by DARPA (Army/AMCOM/REDSTONE AR, W31P4Q-08-1-0009), BES DOE (DE-FG02-07ER46394). JB acknowledges the grant (2009K000192) from the Center for Nanoscale Mechatronics and Manufacturing, one of the 21st Century Frontier Research Programs, supported by the Ministry of Education, Science and Technology, Korea. Work at Brown was supported by the Department of Energy (ER 46387) and The National Science Foundation (0725740). YJC acknowledges support from the Ministry of Knowledge Economy (MKE) and the Korea Industrial Technology Foundation (KOTEF) through the Human Resource Training Project for Strategic Technology.

References

[1] Cui Y and Lieber C M 2001 *Science* **291** 851
[2] Huang Y, Duan X F, Cui Y, Lauhon L J, Kim K H and Lieber C M 2001 *Science* **294** 1313
[3] Ma D D D, Lee C S, Au F C K, Tong S Y and Lee S T 2003 *Science* **299** 1874
[4] Duan X F, Niu C M, Sahi V, Chen J, Parce J W, Empedocles S and Goldman J L 2003 *Nature* **425** 274
[5] Tao A, Kim F, Hess C, Goldberger J, He R R, Sun Y G, Xia Y N and Yang P D 2003 *Nano Lett.* **3** 1229
[6] Whang D, Jin S, Wu Y and Lieber C M 2003 *Nano Lett.* **3** 1255
[7] Ng H T, Han Yamada J T, Nguyen P, Chen Y P and Meyyappan M 2004 *Nano Lett.* **4** 1247
[8] Wagner R S and Ellis W C 1964 *Appl. Phys. Lett.* **4** 89
[9] Tsakalakos L, Balch J, Fronheiser J, Korevaar B A, Sulima O and Rand J 2007 *Appl. Phys. Lett.* **91** 233117
[10] Stelzner T, Pietsch M, Andra G, Falk F, Ose E and Christiansen S 2008 *Nanotechnology* **19** 295203
[11] Peng K Q, Xu Y, Wu Y, Yan Y J, Lee S T and Zhu J 2005 *Small* **1** 1062
[12] Peng K Q, Wang X and Lee S T 2008 *Appl. Phys. Lett.* **92** 163103
[13] Maiolo J R, Kayes B M, Filler M A, Putnam M C, Kelzenberg M D, Atwater H A and Lewis N S 2007 *J. Am. Chem. Soc.* **129** 12346
[14] Fang H, Li X D, Song S, Xu Y and Zhu J 2008 *Nanotechnology* **19** 255703
[15] Kayes B M, Atwater H A and Lewis N S 2005 *J. Appl. Phys.* **97** 11
[16] Kayes B M, Filler M A, Putnam M C, Kelzenberg M D, Lewis N S and Atwater H A 2007 *Appl. Phys. Lett.* **91** 3
[17] Hu L and Chen G 2007 *Nano Lett.* **7** 3249
[18] Brendel R, Bergmann R B, Lolgen P, Wolf M and Werner J H 1997 *Appl. Phys. Lett.* **70** 390
[19] Zhu J, Yu Z F, Burkhard G F, Hsu C M, Connor S T, Xu Y Q, Wang Q, McGehee M, Fan S H and Cui Y 2009 *Nano Lett.* **9** 279
[20] Huang Z P, Fang H and Zhu J 2007 *Adv. Mater.* **19** 744
[21] Ho W S, Lin C H, Cheng T H, Hsu W W, Chen Y Y, Kuo P S and Liu C W 2009 *Appl. Phys. Lett.* **94** 061114
[22] Zhong J, Chen H, Saraf G, Lu Y, Choi C K, Song J J, Mackie M and Shen H 2007 *Appl. Phys. Lett.* **90** 203515
[23] Ono Y, Kimura Y, Ohta Y and Nishida N 1987 *Appl. Opt.* **26** 1142